

Learning Sequential Decisions from Multiple Sources via Group-Robust Markov Decision Processes

Mingyuan Xu¹, Zongqi Xia², Tianxi Cai^{3,4}, Doudou Zhou^{1*}, Nian Si^{5†}

¹Department of Statistics and Data Science, National University of Singapore

²Department of Neurology, University of Pittsburgh

³Department of Biostatistics, Harvard T.H. Chan School of Public Health

⁴Department of Biomedical Informatics, Harvard Medical School

⁵Department of Industrial Engineering and Decision Analytics, Hong Kong University of Science and Technology

Abstract

We often collect data from multiple sites (e.g., hospitals) that share common structure but also exhibit heterogeneity. This paper aims to learn robust sequential decision-making policies from such offline, multi-site datasets. To model cross-site uncertainty, we study distributionally robust MDPs with a group-linear structure: all sites share a common feature map, and both the transition kernels and expected reward functions are linear in these shared features. We introduce feature-wise (d -rectangular) uncertainty sets, which preserve tractable robust Bellman recursions while maintaining key cross-site structure. Building on this, we then develop an offline algorithm based on pessimistic value iteration that includes: (i) per-site ridge regression for Bellman targets, (ii) feature-wise worst-case (row-wise minimization) aggregation, and (iii) a data-dependent pessimism penalty computed from the diagonals of the inverse design matrices. We further propose a cluster-level extension that pools similar sites to improve sample efficiency, guided by prior knowledge of site similarity. Under a robust partial coverage assumption, we prove a suboptimality bound for the resulting policy. Overall, our framework addresses multi-site learning with heterogeneous data sources and provides a principled approach to robust planning without relying on strong state-action rectangularity assumptions.

Keywords: distributionally robust offline reinforcement learning, d -rectangular uncertainty set, pessimistic value iteration, robust partial coverage

*Corresponding author. Email: ddzhou@nus.edu.sg

†Corresponding author. Email: niansi@ust.hk

1 Introduction

Reinforcement learning (RL) provides a general framework for sequential decision making, commonly formalized as a Markov decision process (MDP). In offline RL, policies are learned from pre-collected datasets without further interaction with the environment. This paradigm is significant for high-stakes applications such as healthcare and finance, where ethical, safety, regulatory, and cost considerations preclude online data collection (Pricope, 2021; Zhou et al., 2024). However, the offline trajectories are generated by behavior policies and may provide insufficient coverage of the state–action distribution induced by the optimal policy. This mismatch is referred to as distributional shift, which is a fundamental challenge in offline RL (Levine et al., 2020).

Moreover, real-world datasets are often assembled from multiple sources or sites. Although these sources share a common application context, variation in data-acquisition protocols, population composition, and environmental conditions induces systematic site-wise heterogeneity. For example, hospitals may operate under different formulary restrictions, resulting in site-specific action availability (Zhou et al., 2024). From a statistical perspective, such heterogeneity violates the assumption that trajectories are generated from a fixed MDP and introduce uncertainty regarding the underlying MDP. This suggests the adoption of distributionally robust optimization (DRO), which optimizes the worst-case performance over a plausible uncertainty set.

Methodologically, following group DRO (Sagawa et al., 2020), which models the training distribution via the convex hull of group distributions, a natural way to model the ambiguity in our setting is to consider a cross-site convex hull uncertainty set. However, directly constructing mixtures of site-specific models couples uncertainty across states, actions, and even features, leading to a non-rectangular uncertainty set. In this case, standard dynamic programming breaks, and even planning over Markov deterministic policies is NP-hard (Li, 2025). To formulate a tractable approximation, we adopt a feature-wise rectangular (d -rectangular) uncertainty set that permits independent worst-case choices per feature coordinate. This relaxation restores robust Bellman recursions while preserving key cross-site heterogeneity. Based on this formulation, we develop an offline algorithm using robust value iteration and derive finite-sample suboptimality bounds in the multi-site setting.

1.1 Related Work

In the field of offline RL with standard MDPs, a line of studies design pessimism- (or conservatism-) based methods to mitigate distributional shift under limited data coverage. Model-free approaches include CQL (Kumar et al., 2020), PEVI (Jin et al., 2021) and R-LSVI (Zhang et al., 2022) for corrupted datasets. For model-based algorithms, related studies include MOReL (Kidambi et al., 2020), MOPO (Yu et al., 2020), and CPPO (Uehara and Sun, 2021). Our work adopts the pessimistic value iteration principle of PEVI (Jin et al., 2021), where an uncertainty quantifier serves as a penalty term, and considers a distributionally robust MDP formulation rather than a single nominal linear MDP.

Formally, robust formulation can be viewed as a two-player zero-sum game between an agent and an adversary (Iyengar, 2005). Classical robust MDPs under (s, a) - or s -rectangular uncertainty sets are tractable but often conservative, as the adversary can perturb transitions/rewards independently across states. To reduce conservativeness while maintaining tractability, Goyal and Grand-Clément (2023) propose a d -rectangular¹ uncertainty set, and prove the existence of a deterministic optimal robust policy under this structure.

Building on this robust formulation, recent works design offline algorithms with performance guarantees over tractable uncertainty sets. Ma et al. (2023) design an algorithm with linear function approximation for a d -rectangular uncertainty set, where the transition kernel is linear in known features and the per-feature factors are constrained within divergence balls around their nominal factors. Blanchet et al. (2023) propose a method that combines flexible model estimation with a doubly pessimistic policy optimization step. Their main analysis is developed under (s, a) -rectangular uncertainty set and further covers d -rectangular models defined in the same manner as Ma et al. (2023). Additionally, Liu and Xu (2025) employ transition-targeted ridge regression for robust RL in the linear mixture setting. Complementing these studies, Li et al. (2025) focus on a distributionally robust average-reward offline RL framework and they construct the uncertainty set of state-action-next-state distribution based on the large deviations principle, leading to a non-rectangular structure. They address the resulting problem by adopting an approximate actor-critic algorithm. In contrast to these constructions, we propose a d -rectangular uncertainty set via a feature-wise

¹Referred to as r -rectangularity in Goyal and Grand-Clément (2023).

cross-site convex hull over site-specific factors, capturing the site-wise heterogeneity.

In supervised learning, [Sagawa et al. \(2020\)](#) show that models relying on spurious correlations may suffer high loss on specific data groups, and then study group DRO to minimize the worst-case loss over groups. They further emphasize the importance of regularization in improving the worst-group accuracy for overparameterized models. [Wang et al. \(2024\)](#) propose MIMAL, a framework for measuring variable importance from heterogeneous sources via adversarial learning that maximizes the worst-case predictive reward across source mixtures. These works highlight the role of minimax formulations in multi-source robustness.

Specific to multi-source RL, [Zhou et al. \(2024\)](#) formalize a multi-site linear MDP that separates shared and site-specific effects. They propose a privacy-preserving procedure and incorporate pessimism for reliable policy improvement. Their work is based on a standard linear MDP rather than a robust formulation. [Zhang et al. \(2025\)](#) study zero-shot transfer RL from multiple sources, construct conservative proxies via uncertainty sets and design distributed algorithms with convergence guarantees. Notably, their algorithms rely on updates over the full state-action space, which is stronger than the offline RL setting considered in our study.

1.2 Our Contributions

In this paper, we study offline RL in the multi-site setting, which is complicated by distributional shift and site-wise heterogeneity. To address these challenges, we propose a DRO framework that models cross-site uncertainty and maintains tractability. We formulate the multi-site offline RL problem as a group-linear Distributionally Robust MDP (DRMDP). Specifically, we construct a d -rectangular uncertainty set via a feature-wise cross-site convex hull over site-specific factors. This model can reflect the cross-site heterogeneity while keeping tractability due to its rectangular structure. Building on this formulation, we design an offline algorithm for the group-linear DRMDP that communicates only aggregated site-level summary statistics rather than raw trajectories. This design can reduce the data communication costs and enhance data privacy by avoiding raw data sharing. We further extend this algorithm to a cluster-level variant by merging sites with similarity to improve the sample efficiency. Finally, we derive a decomposition of the suboptimality upper bound and establish performance guarantees for the proposed algorithm.

2 Model and Method

2.1 Multi-Site Linear MDP and Offline Data

We start by fixing notation. For an integer n , let $[n] := \{1, \dots, n\}$, and let $\Delta^{n-1} = \{v \in \mathbb{R}^n : v \geq 0, \|v\|_1 = 1\}$ denote the probability simplex. \mathbf{I}_d denotes the $d \times d$ identity matrix. For a matrix \mathbf{M} , we let $(\mathbf{M})_{ii}$ denote its i -th diagonal entry. For symmetric matrices $\mathbf{A}, \mathbf{B} \in \mathbb{R}^{d \times d}$, we say $\mathbf{A} \succeq \mathbf{B}$ if $\mathbf{A} - \mathbf{B}$ is positive semidefinite, and $\mathbf{A} \succ \mathbf{B}$ if $\mathbf{A} - \mathbf{B}$ is positive definite. For $x, y \in \mathbb{R}$, we define $\min\{x, y\}^+ = \max\{\min\{x, y\}, 0\}$. We use $O(\cdot)$ notation to hide absolute constant factors.

In the multi-site setting, we consider K sites. The underlying MDP of each site $k \in [K]$ is an episodic MDP $(\mathcal{S}, \mathcal{A}, H, \mathcal{P}^k, r^k)$, where \mathcal{S} is the state space, \mathcal{A} is a finite action set, and H is the horizon. The transition kernels $\mathcal{P}^k = \{P_h^k\}_{h=1}^H$ represent the system dynamics, where for each $h \in [H]$ and $(s, a) \in \mathcal{S} \times \mathcal{A}$, $P_h^k(\cdot | s, a)$ is a probability measure on \mathcal{S} . The expected reward functions $r^k = \{r_h^k\}_{h=1}^H$ are deterministic, where $r_h^k : \mathcal{S} \times \mathcal{A} \rightarrow [0, 1]$. The realized reward $R_h^k \in [0, 1]$ satisfies $\mathbb{E}[R_h^k(s_h, a_h) | s_h = s, a_h = a] = r_h^k(s, a)$ for all $h \in [H]$.

Moreover, we assume that each underlying MDP is a linear MDP (see, e.g., Jin et al., 2020, 2021) with a shared and known feature map $\phi : \mathcal{S} \times \mathcal{A} \rightarrow \mathbb{R}^d$. For each step $h \in [H]$ and site $k \in [K]$, there exist unknown probability measures $\boldsymbol{\mu}_h^k = (\mu_{h,1}^k, \dots, \mu_{h,d}^k)^\top$ over \mathcal{S} and an unknown vector $\boldsymbol{\theta}_h^k = (\theta_{h,1}^k, \dots, \theta_{h,d}^k)^\top \in [0, 1]^d$ such that for all $(s, a) \in \mathcal{S} \times \mathcal{A}$,

$$P_h^k(\cdot | s, a) = \langle \phi(s, a), \boldsymbol{\mu}_h^k(\cdot) \rangle, \quad r_h^k(s, a) = \langle \phi(s, a), \boldsymbol{\theta}_h^k \rangle. \quad (1)$$

When \mathcal{S} is continuous, we additionally assume each $\mu_{h,i}^k$ is absolutely continuous with respect to the Lebesgue measure, with density (by abuse of notation) denoted by $\mu_{h,i}^k(s')$. Then $P_h^k(\cdot | s, a)$ admits a density $P_h^k(s' | s, a)$ such that

$$P_h^k(s' | s, a) = \sum_{i=1}^d \phi_i(s, a) \mu_{h,i}^k(s') = \langle \phi(s, a), \boldsymbol{\mu}_h^k(s') \rangle \quad \text{for a.e. } s' \in \mathcal{S}.$$

Moreover, we assume $\int_{\mathcal{S}} \|\boldsymbol{\mu}_h^k(s')\|_2 ds' \leq \sqrt{d}$ for all $h \in [H]$ and $k \in [K]$. From the definition of $\boldsymbol{\theta}_h^k$, we have $\|\boldsymbol{\theta}_h^k\|_2 \leq \sqrt{d}$ for all $h \in [H]$ and $k \in [K]$.

Remark 1 (Simplex features). In addition to the above, we impose a simplex constraint on the features: $\phi(s, a) \in \Delta^{d-1}$ for all (s, a) , i.e., $\phi_i(s, a) \geq 0$ and $\|\phi(s, a)\|_1 = 1$. Consequently, $\|\phi(s, a)\|_2 \leq 1$.

In the offline RL, the learner does not interact with the environments and only has access to $\mathcal{D} = \{\mathcal{D}_k\}_{k=1}^K$, where \mathcal{D}_k contains N_k trajectories collected a priori at site k :

$$\mathcal{D}_k = \left\{ (s_h^{(k,\tau)}, a_h^{(k,\tau)}, r_h^{(k,\tau)}, s_{h+1}^{(k,\tau)}) \right\}_{\tau=1, h=1}^{N_k, H}.$$

Specifically, at each step $h \in [H]$, site $k \in [K]$, and trajectory $\tau \in [N_k]$, $a_h^{(k,\tau)}$ is chosen by a (possibly unknown) behavior policy, and the reward and next state are then generated by the underlying MDP $(\mathcal{S}, \mathcal{A}, H, \mathcal{P}^k, r^k)$ at site k , whose transition kernels and expected reward functions are defined in (1).

2.2 Robust Formulation and Learning Objective

To mitigate the distributional shift and site-wise heterogeneity described in Section 1, we adopt a distributionally robust MDP framework, where at each step h , an adversary selects a transition kernel and reward function from an uncertainty set \mathcal{U}_h to model the worst-case environmental shift.

Formally, we denote the finite-horizon robust MDP by $(\mathcal{S}, \mathcal{A}, H, \{\mathcal{U}_h\}_{h=1}^H)$, where the transitions and rewards are included in the uncertainty set. For each $h \in [H]$, the uncertainty set \mathcal{U}_h is defined in a feature-wise (d -rectangular) form. Specifically, the uncertainty allows for an adversarial choice of the mixing weights over the sites, independently for each feature dimension:

$$\begin{aligned} \mathcal{U}_h = \left\{ (P_h, r_h) : \exists \{ \boldsymbol{\alpha}_{h,i} \in \Delta^{K-1} \}_{i=1}^d \text{ s.t. for all } (s, a), \right. \\ r_h(s, a) = \sum_{i=1}^d \phi_i(s, a) \sum_{k=1}^K \alpha_{h,i}^k \theta_{h,i}^k, \\ \left. P_h(\cdot \mid s, a) = \sum_{i=1}^d \phi_i(s, a) \sum_{k=1}^K \alpha_{h,i}^k \mu_{h,i}^k(\cdot) \right\}. \end{aligned} \quad (2)$$

Here, $\boldsymbol{\alpha}_{h,i} = (\alpha_{h,i}^1, \dots, \alpha_{h,i}^K)^\top$ denotes the mixing weight vector for the i -th feature, which is independent of the state-action pair (s, a) .

In summary, this feature-wise (d -rectangular) construction serves two key purposes. First, it preserves site-wise heterogeneity. As modeled in Section 2.1, where each site has distinct atoms $\{(\boldsymbol{\theta}_h^k, \boldsymbol{\mu}_h^k)\}$, our uncertainty set allows the adversary to select a mixture $\boldsymbol{\alpha}_{h,i}$ independently for each feature. The worst-case backup can draw on any site configuration, preserving

the heterogeneity across sites. Simultaneously, we constrain the rewards and transition kernels to share the same mixture parameters $\alpha_{h,i}$ for each (h, i) . Otherwise, allowing separate mixtures would grant the adversary excessive power to choose them independently, thereby generating overly conservative worst-case estimates.

Given a policy $\pi = \{\pi_h\}_{h=1}^H$, the robust value function V_h^π and Q-function Q_h^π at step h are defined as:

$$V_h^\pi(s) = \inf_{\{(P_t, r_t)\}_{t=h}^H \in \prod_{t=h}^H \mathcal{U}_t} \mathbb{E}_{\{P_t\}_{t=h}^H, \pi} \left[\sum_{t=h}^H r_t(s_t, a_t) \mid s_h = s \right], \quad (3)$$

$$Q_h^\pi(s, a) = \inf_{\{(P_t, r_t)\}_{t=h}^H \in \prod_{t=h}^H \mathcal{U}_t} \mathbb{E}_{\{P_t\}_{t=h}^H, \pi} \left[\sum_{t=h}^H r_t(s_t, a_t) \mid s_h = s, a_h = a \right]. \quad (4)$$

In (3), starting from state s at time h , the agent follows π while an adversary, at each future step $t \geq h$, picks a model $(P_t, r_t) \in \mathcal{U}_t$ to minimize the agent's expected return. The outer infimum captures this worst-case choice. The definition of $Q_h^\pi(s, a)$ in (4) is analogous, with the action a_h fixed to a .

Based on the definitions in (3) and (4), we have the following proposition describing the robust dynamic programming principle. The proof can be found in Supplementary A.1.

Proposition 1 (Robust Bellman Equations). *Under the d -rectangular uncertainty sets $\{\mathcal{U}_h\}_{h=1}^H$, for any policy π , the functions V_h^π and Q_h^π satisfy the following recursive relationships:*

$$Q_h^\pi(s, a) = \inf_{(P_h, r_h) \in \mathcal{U}_h} \{r_h(s, a) + \mathbb{E}_{s' \sim P_h(\cdot|s, a)} [V_{h+1}^\pi(s')] \}, \quad (5)$$

$$V_h^\pi(s) = \mathbb{E}_{a \sim \pi_h(\cdot|s)} [Q_h^\pi(s, a)] = \langle Q_h^\pi(s, \cdot), \pi_h(\cdot \mid s) \rangle_{\mathcal{A}}. \quad (6)$$

Equations (5) and (6) reflect the rectangularity property of the uncertainty set. Specifically, the infimum over the entire future trajectory $\{(P_t, r_t)\}_{t \geq h}$ can be decomposed into a local infimum over $(P_h, r_h) \in \mathcal{U}_h$ at the current step and the value function V_{h+1}^π representing the worst-case future return.

From Proposition 1, we can derive the Q-function of our uncertainty set defined in (2). Since the objective is linear over the simplex and the infimum is attained at a vertex, we use the property $\inf_{\alpha \in \Delta^{K-1}} \sum_{k=1}^K \alpha^{(k)} z_k = \min_{k \in [K]} z_k$. Furthermore, using the fact that $\phi_i(s, a) \geq 0$ for all i , we can interchange the infimum and the summation over features. We

obtain:

$$\begin{aligned}
Q_h^\pi(s, a) &= \inf_{(P_h, r_h) \in \mathcal{U}_h} [r_h(s, a) + \mathbb{E}_{s' \sim P_h(\cdot | s, a)} [V_{h+1}^\pi(s')]] \\
&= \inf_{\{\alpha_{h,i} \in \Delta^{K-1}\}_i} \left[\sum_{i=1}^d \phi_i(s, a) \sum_{k=1}^K \alpha_{h,i}^k \theta_{h,i}^k + \int_{\mathcal{S}} \sum_{i=1}^d \phi_i(s, a) \sum_{k=1}^K \alpha_{h,i}^k \mu_{h,i}^k(s') V_{h+1}^\pi(s') \, ds' \right] \\
&= \sum_{i=1}^d \phi_i(s, a) \inf_{\alpha_{h,i} \in \Delta^{K-1}} \sum_{k=1}^K \alpha_{h,i}^k \left[\theta_{h,i}^k + \int_{\mathcal{S}} \mu_{h,i}^k(s') V_{h+1}^\pi(s') \, ds' \right] \\
&= \sum_{i=1}^d \phi_i(s, a) \min_{k \in [K]} [\theta_{h,i}^k + \langle \mu_{h,i}^k, V_{h+1}^\pi \rangle], \tag{7}
\end{aligned}$$

where we define the inner product $\langle \mu, V \rangle := \int_{\mathcal{S}} V(s') \mu(s') \, ds'$ consistent with the density notation. Hence, the robust Bellman operator can be written as

$$(\mathbb{B}_h V)(s, a) = \sum_{i=1}^d \phi_i(s, a) \min_{k \in [K]} [\theta_{h,i}^k + \langle \mu_{h,i}^k, V \rangle] = \phi(s, a)^\top \mathbf{w}_h, \tag{8}$$

where $\mathbf{w}_h \in \mathbb{R}^d$ is a vector with entries

$$w_{h,i} = \min_{k \in [K]} [\theta_{h,i}^k + \langle \mu_{h,i}^k, V \rangle], \quad i \in [d]$$

This result indicates that for any fixed value function V , the robust Bellman operator preserves the linear structure with respect to the feature map ϕ .

After introducing the robust formulation, we now state our learning objective. Let

$$\Pi := \left\{ \pi = \{\pi_h\}_{h=1}^H : \pi_h(\cdot | s) \in \Delta(\mathcal{A}) \text{ for all } (s, h) \right\}$$

denote the class of Markov (possibly randomized) policies ². Recall the definition of robust value function in (3). We define the robust optimal value function as

$$V_h^*(s) := \sup_{\pi \in \Pi} V_h^\pi(s), \quad \forall h \in [H], \forall s \in \mathcal{S}.$$

Let $\pi^* \in \Pi$ be an optimal robust policy such that

$$V_h^*(s) = V_h^*(s), \quad \forall h \in [H], \forall s \in \mathcal{S},$$

²For robust MDPs with d -rectangular uncertainty sets, an optimal Markov policy exists and can be chosen deterministic in the infinite-horizon setting (Goyal and Grand-Clément, 2023). In our finite-horizon setting with the product uncertainty model $\prod_{h=1}^H \mathcal{U}_h$, the same conclusion follows from robust backward induction. We allow randomized Markov policies for notational convenience.

where the proof of the existence is provided in Supplementary A.2. Given an estimator $\hat{\pi} \in \Pi$ learned from the offline dataset \mathcal{D} , we measure its (robust) suboptimality by

$$\text{SubOpt}(\hat{\pi}; s) := V_1^{\pi^*}(s) - V_1^{\hat{\pi}}(s), \quad s \in \mathcal{S}. \quad (9)$$

Our goal is to design an offline robust RL procedure that, using only pre-collected dataset, outputs a policy with provably controlled suboptimality.

2.3 Algorithm

We implement robust offline RL by introducing a data-dependent penalty inside the feature-wise (d-rectangular) Bellman backup, inspired by the pessimism principle in [Jin et al. \(2021\)](#). In our algorithm, we estimate the Bellman backup $(\mathbb{B}_h \hat{V}_{h+1})(s, a)$ rather than the operator \mathbb{B}_h itself. Given the offline dataset \mathcal{D} , we construct an estimated backup $(\hat{\mathbb{B}}_h \hat{V}_{h+1})(s, a)$ that approximates $(\mathbb{B}_h \hat{V}_{h+1})(s, a)$, where $\hat{V}_{h+1} : \mathcal{S} \rightarrow \mathbb{R}$ is computed by the algorithm.

First, we provide the definition of ξ -uncertainty quantifier with the confidence parameter $\xi \in (0, 1)$:

Definition 1 (ξ -uncertainty quantifier ([Jin et al., 2021](#))). A collection $\{\Gamma_h\}_{h=1}^H$, with $\Gamma_h : \mathcal{S} \times \mathcal{A} \rightarrow \mathbb{R}_+$, is a ξ -uncertainty quantifier (with respect to $\mathbb{P}_{\mathcal{D}}$) if the event

$$\mathcal{E} = \left\{ |(\hat{\mathbb{B}}_h \hat{V}_{h+1})(s, a) - (\mathbb{B}_h \hat{V}_{h+1})(s, a)| \leq \Gamma_h(s, a), \forall (s, a), \forall h \in [H] \right\} \quad (10)$$

satisfies $\mathbb{P}_{\mathcal{D}}(\mathcal{E}) \geq 1 - \xi$.

Based on the Bellman operator defined in Equation (8), we construct $\hat{\mathbb{B}}_h \hat{V}_{h+1}$ based on the dataset \mathcal{D} as follows. For each site $k \in [K]$ and step $h \in [H]$, we define the Bellman target as

$$y_h^{(k, \tau)} := r_h^{(k, \tau)} + \hat{V}_{h+1} \left(s_{h+1}^{(k, \tau)} \right),$$

and the empirical mean-squared Bellman error (MSBE) ([Jin et al., 2021](#)) as

$$M_h^k(\boldsymbol{\nu}) := \sum_{\tau=1}^{N_k} \left(y_h^{(k, \tau)} - \phi(s_h^{(k, \tau)}, a_h^{(k, \tau)})^\top \boldsymbol{\nu} \right)^2.$$

We then estimate the site-wise coefficient vector by ridge regression:

$$\hat{\boldsymbol{\nu}}_h^k = \arg \min_{\boldsymbol{\nu} \in \mathbb{R}^d} M_h^k(\boldsymbol{\nu}) + \lambda \|\boldsymbol{\nu}\|_2^2 \implies \hat{\boldsymbol{\nu}}_h^k = (\Lambda_h^k)^{-1} \sum_{\tau=1}^{N_k} \phi(s_h^{(k, \tau)}, a_h^{(k, \tau)}) y_h^{(k, \tau)}, \quad (11)$$

where

$$\Lambda_h^k = \sum_{\tau=1}^{N_k} \phi(s_h^{(k,\tau)}, a_h^{(k,\tau)}) \phi(s_h^{(k,\tau)}, a_h^{(k,\tau)})^\top + \lambda \cdot \mathbf{I}_d.$$

For vectors $\{v^k\}_{k=1}^K \subset \mathbb{R}^d$, we define the coordinate-wise minimum and maximum operators as

$$\text{rowmin}\{v^1, \dots, v^K\} := \left(\min_{k \in [K]} v_i^k\right)_{i=1}^d, \quad \text{rowmax}\{v^1, \dots, v^K\} := \left(\max_{k \in [K]} v_i^k\right)_{i=1}^d.$$

By (8), the population backup is a feature-wise minimum over sites. We mirror this by the row-wise minimum

$$\widehat{\mathbf{w}}_h := \text{rowmin}\{\widehat{\boldsymbol{\nu}}_h^1, \dots, \widehat{\boldsymbol{\nu}}_h^K\} \in \mathbb{R}^d, \quad (\widehat{\mathbf{w}}_h)_i = \min_{k \in [K]} (\widehat{\boldsymbol{\nu}}_h^k)_i, \quad \forall i \in [d],$$

and define the plug-in (no penalty) backup as

$$(\widehat{\mathbb{B}}_h \widehat{V}_{h+1})(s, a) := \boldsymbol{\phi}(s, a)^\top \widehat{\mathbf{w}}_h. \quad (12)$$

Meanwhile, we construct the data-dependent pessimism term. For each site k , let $\mathbf{d}_h^k = \text{diag}((\Lambda_h^k)^{-1}) \in \mathbb{R}^d$ and $\mathbf{s}_h^k = \sqrt{\mathbf{d}_h^k} \in \mathbb{R}^d$ (element-wise). We aggregate the per-feature uncertainties by defining

$$\mathbf{m}_h := \text{rowmax}\{\mathbf{s}_h^1, \dots, \mathbf{s}_h^K\} \in \mathbb{R}^d, \quad (\mathbf{m}_h)_i = \max_{k \in [K]} (\mathbf{s}_h^k)_i, \quad \forall i \in [d].$$

For a scaling parameter $\beta > 0$, we define the uncertainty quantifier as

$$\begin{aligned} \Gamma_h(s, a) &:= \beta \langle \boldsymbol{\phi}(s, a), \mathbf{m}_h \rangle = \beta \sum_{i=1}^d \phi_i(s, a) \max_{k \in [K]} \sqrt{((\Lambda_h^k)^{-1})_{ii}} \\ &= \beta \sum_{i=1}^d \max_{k \in [K]} \|\phi_i(s, a) \mathbf{e}_i\|_{(\Lambda_h^k)^{-1}}, \end{aligned} \quad (13)$$

where $\mathbf{e}_i \in \mathbb{R}^d$ is the i -th standard basis vector. In addition, $\|\mathbf{v}\|_{\mathbf{M}} := \sqrt{\mathbf{v}^\top \mathbf{M} \mathbf{v}}$, and since $\phi_i(s, a) \geq 0$, $\|\phi_i(s, a) \mathbf{e}_i\|_{(\Lambda_h^k)^{-1}} = \phi_i(s, a) \sqrt{((\Lambda_h^k)^{-1})_{ii}}$.

Combining the plug-in backup (12) and the uncertainty quantifier (13), we define the pessimistic Q -backup and value update by

$$\overline{Q}_h(s, a) = (\widehat{\mathbb{B}}_h \widehat{V}_{h+1})(s, a) - \Gamma_h(s, a), \quad \widehat{Q}_h(s, a) = \min\{\overline{Q}_h(s, a), H - h + 1\}^+,$$

$$\widehat{\pi}_h(\cdot \mid x) = \arg \max_{\pi_h} \left\langle \widehat{Q}_h(x, \cdot), \pi_h(\cdot \mid x) \right\rangle_{\mathcal{A}}, \quad \widehat{V}_h(s) = \langle \widehat{Q}_h(s, \cdot), \widehat{\pi}_h(\cdot \mid s) \rangle_{\mathcal{A}},$$

with $\widehat{V}_{H+1} \equiv 0$. The complete procedure is summarized in Algorithm 1.

Algorithm 1 Pessimistic site-wise ridge with feature-wise uncertainty

Require: features $\phi : \mathcal{S} \times \mathcal{A} \rightarrow \mathbb{R}^d$, horizon H , regularizer $\lambda = 1$, datasets $\mathcal{D} = \{\mathcal{D}_k\}_{k=1}^K$

with $\mathcal{D}_k = \{(s_h^{(k,\tau)}, a_h^{(k,\tau)}, r_h^{(k,\tau)}, s_{h+1}^{(k,\tau)})\}_{\tau=1, h=1}^{N_k, H}$.

```

1:  $\widehat{V}_{H+1}(\cdot) \leftarrow 0$ 
2: for  $h = H, H-1, \dots, 1$  do
3:   (A) Site-wise ridge for next-state values; collect diag-inverse norms
4:   for  $k = 1$  to  $K$  do
5:      $\Lambda_h^k \leftarrow \sum_{\tau=1}^{N_k} \phi(s_h^{(k,\tau)}, a_h^{(k,\tau)}) \phi(s_h^{(k,\tau)}, a_h^{(k,\tau)})^\top + \lambda \cdot \mathbf{I}_d$ 
6:      $\widehat{\boldsymbol{\nu}}_h^k \leftarrow (\Lambda_h^k)^{-1} \left( \sum_{\tau=1}^{N_k} \phi(s_h^{(k,\tau)}, a_h^{(k,\tau)}) (r_h^{(k,\tau)} + \widehat{V}_{h+1}(s_{h+1}^{(k,\tau)})) \right)$ 
7:      $\mathbf{d}_h^k \leftarrow \text{diag}((\Lambda_h^k)^{-1}) \in \mathbb{R}^d$ 
8:      $\mathbf{s}_h^k \leftarrow \sqrt{\mathbf{d}_h^k} \in \mathbb{R}^d$  ▷  $[\mathbf{s}_h^k]_i = \|\mathbf{e}_i\|_{(\Lambda_h^k)^{-1}}$ 
9:   end for
10:  (Row-min/max across sites)
11:  for  $i = 1$  to  $d$  do
12:     $(\widehat{\mathbf{w}}_h)_i \leftarrow \min_{k \in [K]} (\widehat{\boldsymbol{\nu}}_h^k)_i$ 
13:     $(\mathbf{m}_h)_i \leftarrow \max_{k \in [K]} (\mathbf{s}_h^k)_i$ 
14:  end for
15:  (B) Compute  $Q/\pi/V$  with data-dependent pessimism
16:   $\overline{Q}_h(\cdot, \cdot) \leftarrow \langle \phi(\cdot, \cdot), \widehat{\mathbf{w}}_h \rangle - \beta \langle \phi(\cdot, \cdot), \mathbf{m}_h \rangle$ 
17:   $\widehat{Q}_h(\cdot, \cdot) \leftarrow \min \{ \overline{Q}_h(\cdot, \cdot), H - h + 1 \}^+$ 
18:   $\widehat{\pi}_h(\cdot | \cdot) \leftarrow \arg \max_{\pi_h} \left\langle \widehat{Q}_h(\cdot, \cdot), \pi_h(\cdot | \cdot) \right\rangle_{\mathcal{A}}$  ▷ greedy
19:   $\widehat{V}_h(\cdot) \leftarrow \langle \widehat{Q}_h(\cdot, \cdot), \widehat{\pi}_h(\cdot | \cdot) \rangle_{\mathcal{A}}$ 
20: end for
21: Output:  $\widehat{\pi} = \{\widehat{\pi}_h\}_{h=1}^H$ 

```

3 Theory

This section provides the theoretical guarantees for the proposed Algorithm 1. In Section 3.1, we demonstrate the decomposition of suboptimality upper bound for robust MDP. In Section 3.2, we establish a theoretical upper bound for the suboptimality, and derive the corresponding convergence rate with respect to the sample size. In Section 3.3, we extend the proposed algorithm to the cluster level under the cross-site similarity prior knowledge, and provide the theoretical guarantee characterized by the discrepancy metric.

3.1 Decomposition of Suboptimality for Robust MDP

In this section, we upper bound the suboptimality defined in (9) by three terms. Following the terminology of Jin et al. (2021), we refer to them as *spurious correlation*, *intrinsic uncertainty*, and *optimization error*.

In Algorithm 1, based on the offline dataset \mathcal{D} , we construct an estimated Q -function $\widehat{Q}_h : \mathcal{S} \times \mathcal{A} \rightarrow \mathbb{R}$ and an estimated value function $\widehat{V}_h : \mathcal{S} \rightarrow \mathbb{R}$. We then define the (pointwise) model evaluation error at step $h \in [H]$ by

$$\iota_h(s, a) := (\mathbb{B}_h \widehat{V}_{h+1})(s, a) - \widehat{Q}_h(s, a), \quad (14)$$

which captures the discrepancy between applying the true robust Bellman operator to the value \widehat{V}_{h+1} and the estimated Q -value at (s, a) . Note that both \widehat{V}_{h+1} and \widehat{Q}_h depend on \mathcal{D} .

Let $\widehat{\pi} = \{\widehat{\pi}_h\}_{h=1}^H$ satisfy $\widehat{V}_h(s) = \langle \widehat{Q}_h(s, \cdot), \widehat{\pi}_h(\cdot | s) \rangle_{\mathcal{A}}$ for all $s \in \mathcal{S}, h \in [H]$. Then its suboptimality can be upper bounded as follows. The proof can be found in Supplementary A.3.

Lemma 2 (Decomposition of Suboptimality for Robust MDP). *Let $\pi^* \in \Pi$ be an optimal policy, and $\widehat{\pi} = \{\widehat{\pi}_h\}_{h=1}^H$ be the policy induced by the estimators such that $\widehat{V}_h(s) = \langle \widehat{Q}_h(s, \cdot), \widehat{\pi}_h(\cdot | s) \rangle_{\mathcal{A}}$.*

For the initial state $s \in \mathcal{S}$, the suboptimality can be decomposed as:

$$\begin{aligned} \text{SubOpt}(\widehat{\pi}; s) &= V_1^{\pi^*}(s) - V_1^{\widehat{\pi}}(s) \\ &\leq - \underbrace{\sum_{h=1}^H \mathbb{E}^{\widehat{\pi}, P^{\widehat{\pi}, \natural}} [\iota_h(s_h, a_h) \mid s_1 = s]}_{(i): \text{ Spurious Correlation}} \end{aligned}$$

$$\begin{aligned}
& + \underbrace{\sum_{h=1}^H \mathbb{E}^{\pi^*, P^{\pi^*, \dagger}} [\iota_h(s_h, a_h) \mid s_1 = s]}_{(ii): \text{ Intrinsic Uncertainty}} \\
& + \underbrace{\sum_{h=1}^H \mathbb{E}^{\pi^*, P^{\pi^*, \ddagger}} \left[\left\langle \hat{Q}_h(s_h, \cdot), \pi_h^*(\cdot \mid s_h) - \hat{\pi}_h(\cdot \mid s_h) \right\rangle \mid s_1 = s \right]}_{(iii): \text{ Optimization Error}}
\end{aligned}$$

Here $\mathbb{E}^{\pi, P^{\pi^*, \diamond}}[\cdot \mid s_1 = s]$ is the expectation under the trajectory generated by policy π together with the (possibly different) transition kernels $P^{\pi, \diamond} = \{P_h^{\pi, \diamond}\}_{h=1}^H$, with $\diamond \in \{\natural, \dagger, \ddagger\}$ distinguishing the three selections. At each step h , the kernel $P_h^{\pi, \diamond}(\cdot \mid s, a)$ is chosen to attain the supremum in the corresponding robust backup (see Supplementary A.3 for explicit definitions).

As noted by Jin et al. (2021), term (i) is particularly challenging to control because $\hat{\pi}$ and ι_h are both data-dependent, which induces spurious correlation. They further construct a multi-armed bandit example showing that this effect can lead to significant suboptimality. By contrast, term (ii) is easier to control because π^* is determined by the underlying MDP and is independent of the dataset \mathcal{D} , removing the data-dependent coupling that complicates term (i). If, in addition, we choose $\hat{\pi}$ to be stagewise greedy with respect to \hat{Q}_h , i.e.,

$$\hat{\pi}_h(\cdot \mid s) \in \arg \max_{\pi \in \Pi} \langle \hat{Q}_h(s, \cdot), \pi(\cdot) \rangle,$$

then the optimization-error term (iii) will be non-positive.

3.2 Suboptimality Upper Bound

The following theorem characterizes the suboptimality (9) of the resulting policy derived from Algorithm 1. The proof can be found in Supplementary A.4.

Theorem 3 (Suboptimality). *In Algorithm 1, we set*

$$\lambda = 1, \beta = c \cdot dH\sqrt{\zeta}, \text{ and } \zeta = \log(2dKH N_{\max}/\xi)$$

Here $c > 0$ is an absolute constant, $\xi \in (0, 1)$ is the confidence parameter, and $N_{\max} = \max_k N_k$. The following statements hold: for $\hat{\pi}$ in Algorithm 1, we have

$$\text{SubOpt}(\hat{\pi}; s) \leq 2\beta \sum_{h=1}^H \sum_{i=1}^d \mathbb{E}^{\pi^*, P^{\pi^*, \dagger}} \left[\max_k \|\phi_i(s_h, a_h) \mathbf{e}_i\|_{(\Lambda_h^k)^{-1}} \mid s_1 = s \right]$$

holds with probability at least $1 - \xi$, where $\mathbb{E}^{\pi^*, P^{\pi^*, \dagger}}$ is with respect to the trajectory induced by π^* and the transition kernel $P^{\pi^*, \dagger}$. $P^{\pi^*, \dagger}$ denotes a specific transition kernel sequence that relates to the optimal policy π^* .

To convert the expectation in Theorem 3 into an explicit sample-size rate, we impose the following robust partial coverage condition on the feature covariance.

Assumption 1 (Robust partial coverage covariance matrix). For

$$\frac{1}{N_k} \Lambda_h^k = \frac{1}{N_k} \sum_{\tau=1}^{N_k} \phi(s_h^{(k, \tau)}, a_h^{(k, \tau)}) \phi(s_h^{(k, \tau)}, a_h^{(k, \tau)})^\top + \frac{\lambda}{N_k} \mathbf{I}_d$$

we assume that for some constant c^\dagger

$$\frac{1}{N_k} \Lambda_h^k \succeq \frac{\lambda}{N_k} \cdot \mathbf{I}_d + c^\dagger \cdot \mathbb{E}_{(s_h, a_h) \sim d_{P, h}^{\pi^*}} \left[(\phi_i(s_h, a_h) \mathbf{e}_i) (\phi_i(s_h, a_h) \mathbf{e}_i)^\top \right]$$

for any $k \in [K]$, $i \in [d]$, $h \in [H]$, and $P = (P_1, \dots, P_H) \in \prod_{t=1}^H \mathcal{P}_t$ (\mathcal{P}_h is the uncertainty set of transition kernels). Here $d_{P, h}^{\pi^*}$ denotes the step- h state-action visitation distribution induced by policy π^* under the transition kernel $P = \{P_h\}_{h=1}^H$.

This assumption extends the robust partial coverage condition from [Blanchet et al. \(2023, Assumption 6.2\)](#) to our multi-site setting. Specifically, it indicates that, along each coordinate i , the ridge-regularized empirical covariance at site k dominates the corresponding second moment under the robust target occupancy, up to the constant c^\dagger . Similar to [Blanchet et al. \(2023\)](#), we require the dataset to cover the state-action pairs visited by the robust optimal policy under all the transition kernels in the uncertainty set. However, unlike their single-site setting, we enforce this condition on the site-specific covariance matrices Λ_h^k , requiring it to hold for all sites.

Combining Theorem 3 with the robust partial coverage condition in Assumption 1, we derive the following corollary. The proof can be found in Supplementary A.5.

Corollary 4 (Suboptimality with partial coverage). *Under Assumption 1, in Algorithm 1, we set*

$$\lambda = 1, \beta = c \cdot dH\sqrt{\zeta}, \text{ and } \zeta = \log(2dKH N_{\max}/\xi).$$

Here $c > 0$ is an absolute constant, $\xi \in (0, 1)$ is the confidence parameter, $N_{\max} = \max_k N_k$ and $N_{\min} = \min_k N_k$. For $\widehat{\pi}$ in Algorithm 1, we have

$$\text{SubOpt}(\widehat{\pi}; s) \leq c^\dagger d^2 H^2 \sqrt{\frac{\log(dKHN_{\max}/\xi)}{N_{\min}}}$$

holds with probability at least $1 - \xi$, where $c^\dagger > 0$ is an absolute constant that only depends on c^\dagger and c .

3.3 Cross-Site Similarity

Building upon the Algorithm 1, we further generalize our framework to settings exhibiting cross-site similarity, where subsets of sites are known a priori to share similar underlying MDPs. Specifically, suppose the sites are partitioned into M disjoint clusters $\{\mathcal{C}_m\}_{m=1}^M$. In this setting, we treat each cluster as a single “super-site” by aggregating the datasets from all sites within the same cluster.

Formally, for each cluster m , let $\boldsymbol{\nu}_h^m$ denote the cluster-level representative parameter (derived from the underlying parameters of sites in \mathcal{C}_m). We define the *cluster-level robust* Bellman operator as:

$$(\mathbb{B}_h^{\text{pool}} V)(s, a) = \sum_{i=1}^d \phi_i(s, a) \eta_{h,i}(V) = \phi(s, a)^\top \boldsymbol{\eta}_h(V),$$

where the robust target $\boldsymbol{\eta}_h(V)$ is defined by taking the minimum across cluster representatives:

$$\eta_{h,i}(V) := \min_{m \in [M]} \nu_{h,i}^m(V) = \min_{m \in [M]} \left[\theta_{h,i}^m + \int_{\mathcal{S}} V(s') \mu_{h,i}^m(s') ds' \right].$$

Here, $(\boldsymbol{\theta}_h^m, \boldsymbol{\mu}_h^m)$ can be viewed as the centroid of the underlying parameters of sites within cluster \mathcal{C}_m , and represents the pooled parameters for cluster m . Accordingly, the empirical operator is constructed by plugging in the estimators learned from the pooled datasets:

$$(\widehat{\mathbb{B}}_h^{\text{pool}} \widehat{V}_{h+1})(s, a) := \phi(s, a)^\top \widehat{\boldsymbol{\eta}}_h, \quad \text{with} \quad \widehat{\eta}_{h,i} := \min_{m \in [M]} \widehat{\nu}_{h,i}^m,$$

where $\widehat{\nu}_h^m$ is the ridge regression estimator obtained using the aggregated dataset $\mathcal{D}_{\mathcal{C}_m} := \bigcup_{k \in \mathcal{C}_m} \mathcal{D}_k$. Let N_m denote the number of trajectories in each cluster, then $\widehat{\nu}_h^m$ can be expressed as:

$$\widehat{\nu}_h^m = (\Lambda_h^m)^{-1} \sum_{\tau=1}^{N_m} \phi(s_h^{(m,\tau)}, a_h^{(m,\tau)}) \left(r_h^{(m,\tau)} + \widehat{V}_{h+1} \left(s_{h+1}^{(m,\tau)} \right) \right), \quad (15)$$

with

$$\Lambda_h^m = \sum_{\tau=1}^{N_m} \phi(s_h^{(m,\tau)}, a_h^{(m,\tau)}) \phi(s_h^{(m,\tau)}, a_h^{(m,\tau)})^\top + \lambda \cdot \mathbf{I}_d.$$

In addition, the penalty term in this cluster-level algorithm is

$$\Gamma_h^{\text{pool}} = \sum_{i=1}^d \max_m \beta^{\text{pool}} \|\phi_i(s, a) \mathbf{e}_i\|_{(\Lambda_h^m)^{-1}},$$

where β^{pool} is a scaling parameter. To account for the heterogeneity introduced by this approximation, we define the within-cluster parameter discrepancy for each step h and cluster m as:

$$\Delta_{h,m} := \sup_{V \in \mathcal{V}_{h+1}^{\text{pool}}} \max_{k \in \mathcal{C}_m} \|\boldsymbol{\nu}_h^k(V) - \boldsymbol{\nu}_h^m(V)\|_2, \quad \Delta_h = \max_m \Delta_{h,m},$$

where

$$\mathcal{V}_h^{\text{pool}}(R, B, \lambda) = \{V_h(s; \theta, \beta, \Sigma_1, \dots, \Sigma_M) : \mathcal{S} \rightarrow [0, H] \text{ with } \|\theta\| \leq R, \beta \in [0, B], \Sigma_1, \dots, \Sigma_M \succeq \lambda \cdot I\},$$

$$V_h(s; \theta, \beta, \Sigma_1, \dots, \Sigma_M) = \max_{a \in \mathcal{A}} \left\{ \min \left\{ \phi(s, a)^\top \theta - \beta \sum_{i=1}^d \max_{m \in [M]} \|\phi_i(s, a) \mathbf{e}_i\|_{(\Sigma_m)^{-1}}, H - h + 1 \right\}^+ \right\}.$$

Similar to Assumption 1 over the site level, we provide the following assumption.

Assumption 2 (Robust partial coverage covariance matrix over the cluster level). Let π^* be the robust optimal policy. For any $m \in [M]$, $i \in [d]$, $h \in [H]$, and $P = (P_1, \dots, P_H) \in \prod_{t=1}^H \mathcal{P}_t$ (\mathcal{P}_h is the uncertainty set of transition kernels), we assume that there exists a constant c' such that the empirical covariance matrix of cluster m satisfies:

$$\frac{1}{N_m} \Lambda_h^m \succeq \frac{\lambda}{N_m} \cdot \mathbf{I}_d + c' \cdot \mathbb{E}_{(s_h, a_h) \sim d_{P,h}^{\pi^*}} \left[(\phi_i(s_h, a_h) \mathbf{e}_i) (\phi_i(s_h, a_h) \mathbf{e}_i)^\top \right].$$

Remark 2. Assumption 2 can be directly derived from Assumption 1. Specifically, if we assume the site-level coverage holds uniformly such that $\frac{1}{N_k} \Lambda_h^k \succeq \frac{\lambda}{N_k} \cdot \mathbf{I}_d + c^\dagger \cdot \Sigma_{\text{target}}$ for all $k \in \mathcal{C}_m$, then by adding the covariance matrices, the aggregated matrix satisfies:

$$\begin{aligned} \Lambda_h^m &= \lambda \cdot \mathbf{I}_d + \sum_{\tau=1}^{N_m} \phi(s_h^{(m,\tau)}, a_h^{(m,\tau)}) \phi(s_h^{(m,\tau)}, a_h^{(m,\tau)})^\top \\ &= \lambda \cdot \mathbf{I}_d + \sum_{k \in \mathcal{C}_m} \sum_{\tau=1}^{N_k} \phi(s_h^{(k,\tau)}, a_h^{(k,\tau)}) \phi(s_h^{(k,\tau)}, a_h^{(k,\tau)})^\top \\ &\succeq \lambda \mathbf{I}_d + \sum_{k \in \mathcal{C}_m} N_k c^\dagger \cdot \Sigma_{\text{target}} \end{aligned}$$

$$= \lambda \mathbf{I}_d + N_m c^\dagger \cdot \Sigma_{\text{target}}$$

which implies Assumption 2 holding with $c' = c^\dagger$. This highlights that aggregating data from similar sites preserves (and stabilizes) the feature coverage.

Based on Assumption 2, we obtain the following corollary, which upper-bounds the suboptimality of the cluster-level algorithm. The proof can be found in Supplementary A.6.

Corollary 5 (Cluster-Level Suboptimality). *Suppose Assumption 2 holds. Let $\text{Pool}(\mathcal{D})$ be the policy learned via Algorithm 1 using the cluster-aggregated dataset $\mathcal{D} = \bigcup_m \mathcal{D}_{C_m}$. Set*

$$\lambda = 1, \beta^{\text{pool}} = c \cdot dH \sqrt{\zeta^{\text{pool}}}, \text{ and } \zeta^{\text{pool}} = \log(2dMHN_{\max}^{\text{pool}}/\xi)$$

Here $c > 0$ is an absolute constant, $\xi \in (0, 1)$ is the confidence parameter, $N_{\max}^{\text{pool}} = \max_m N_m$, and $N_{\min}^{\text{pool}} = \min_m N_m$. Then the suboptimality of $\text{Pool}(\mathcal{D})$ at state $s \in \mathcal{S}$ satisfies

$$\text{SubOpt}(\text{Pool}(\mathcal{D}); s) \leq c^\natural d^2 H^2 \sqrt{\frac{\log(dMHN_{\max}^{\text{pool}}/\xi)}{N_{\min}^{\text{pool}}}} + C^\natural \sum_{h=1}^H \Delta_h,$$

with probability at least $1 - \xi$. Here, $c^\natural > 0$ is a constant depending on c and c^\dagger , and the bias coefficient is given by

$$C^\natural = 2 \left(\sup_{(s,a)} \sum_{i=1}^d \phi_i(s, a) \sqrt{\frac{d}{c' \sigma_i^2}} + 1 \right),$$

where $\sigma_i^2 = \mathbb{E}_{(s_h, a_h) \sim d_{P,h}^{\pi^*}} [\phi_i(s_h, a_h)^2]$ represents the feature coverage under the robust optimal policy.

Remark 3. The coefficient C^\natural in Corollary 5 characterizes how the structural discrepancy Δ_h is propagated through the feature space, determined by c' and σ_i jointly. While σ_i quantifies the importance of the i -th feature dimension under the robust optimal policy π^* , c' scales the minimum effective coverage provided by the pooled covariance matrix. This joint formulation helps the bound remain adaptive. In sparse feature regions where σ_i^2 is small, a modest amount of pooled data may still yield a sufficiently large c^\dagger to suppress the propagation of Δ_h , thereby maintaining the stability of the global suboptimality.

Corollary 5 highlights the theoretical advantage of aggregating similar sites. While Corollary 4 shows that the site-wise algorithm suffers from high estimation variance due to limited local sample sizes (controlled by N_{\min}), the cluster-level algorithm leverages the pooled

sample size N_{\min}^{pool} (where $N_{\min}^{\text{pool}} \geq N_{\min}$) to suppress this error. Consequently, as long as the within-cluster heterogeneity Δ_h is controlled, specifically when $\Delta_h \ll O(1/\sqrt{N_{\min}} - 1/\sqrt{N_{\min}^{\text{pool}}})$, the cluster-level estimator achieves a lower suboptimality upper bound. This formally justifies pooling strategies in multi-site settings where sites share common structures but individual data coverage is limited.

4 Simulation

4.1 Multi-site Performance Comparison

In this section, we evaluate the performance of Algorithm 1 in the multi-site setting by comparing it against the following competitive benchmarks:

- **Naive Pooling:** The dataset from all sites are aggregated and treated as a single dataset. The Pessimistic Value Iteration (PEVI) algorithm (Jin et al., 2021) is then applied directly to this pooled dataset to learn the policy.
- **Per-Site PEGI (Average- Q):** The PEGI algorithm is run independently on the dataset from each site. The resulting site-specific Q -functions are then averaged, and the greedy policy is derived from this average Q -function.
- **Per-Site PEGI (Min- Q):** The PEGI algorithm is run independently on the dataset from each site. The final Q -function is taken as the pointwise minimum across all site-specific Q -functions, and the greedy policy is derived from this conservative Q -estimate.

We simulate data from episodic linear MDPs for $K = 3$ different sites. The state space is $\mathcal{S} \subseteq [0, 1]^p$, where $p = 3$ denotes the state dimension, and the action set \mathcal{A} is finite, where $|\mathcal{A}| = 10$. The horizon length is $H = 7$. The feature map $\phi(s, a) \in \mathbb{R}^d$ is structured to be sparse and action-specific. Specifically, for any state-action pair (s, a) , we first form a nonnegative, ℓ_1 -normalized version of the state vector, and then insert it into the block corresponding to action a , while setting all other action blocks to zero. The dimension of the resulting feature map is $p \times |\mathcal{A}|$.

For each site $k \in [K]$ and step $h \in [H]$, we assume the expected reward function and transition kernel adhere to the linear forms specified in Section 2.1. For each site k , the degree of heterogeneity across sites is controlled by systematically perturbing the global parameter sets $\{(\boldsymbol{\theta}_h^k, \boldsymbol{\mu}_h^k)\}_{h=1}^H$. For each $(k, h, i) \in [K] \times [H] \times [d]$, we generate the component $\theta_{h,i}^k$ independently from uniform distribution on $[0.1, 0.9]$. For the transition components $\{\mu_{h,i}^k\}_{i=1}^d$, we assume conditional independence across state dimensions and model each dimension of s' by a Beta distribution with parameters $(\alpha_{k,h,i,j}, \beta_{k,h,i,j})$ ($j \in [p]$). These parameters are generated by considering both site-level and step-level heterogeneity and are lower-bounded by a constant to ensure numerical stability. We then generate N_k independent trajectories under a uniformly random behavior policy (i.e., at each step the action is sampled uniformly from \mathcal{A} , independently of the state), with initial states sampled uniformly from \mathcal{S} . All rewards are clipped to the interval $[0, 1]$, and states are constrained to remain within $[0, 1]^p$.

We evaluate the four methods listed above using the following common parameters: the ridge regularization coefficient is set to $\lambda = 1$, the confidence level for uncertainty quantification is $\xi = 0.05$, and the scaling constant in the penalty term is $c = 5 \times 10^{-4}$. The number of offline trajectories for the three sites are set to $N_1 = 3000$, $N_2 = 2000$, and $N_3 = 5000$, respectively. The performance metric is the robust suboptimality defined in (9). To compute the optimal robust value $V_1^*(s)$, we perform backward induction starting from $V_{H+1}^*(s) \equiv 0$. We apply the robust Bellman optimality operator to obtain V_h^* and derive the optimal policy $\pi_h^*(s) \in \arg \max_{a \in \mathcal{A}} Q_h^*(s, a)$ at each step h . For learned policies $\widehat{\pi}$, the robust values $V_1^{\widehat{\pi}}$ are computed via a similar backward recursion using the robust policy evaluation operator, where the action at each step is determined by $\widehat{\pi}$.

To evaluate the performance of each method, we conduct $R = 50$ independent trials using different random seeds. In each trial, we estimate the expected suboptimality by averaging over $m = 200$ initial states sampled uniformly from \mathcal{S} . We then report the mean and the 95% confidence interval of these R average suboptimality values. As illustrated in the Figure 1, Algorithm 1 consistently achieves significantly lower suboptimality compared to the benchmark methods. In contrast, the Naive Pooling method exhibits substantial robust suboptimality. This is expected because pooling inherently optimizes for the average performance across the aggregated distribution, thereby ignoring the worst-case scenarios within the uncertainty set. Consequently, the pooled policy fails to be robust against site-

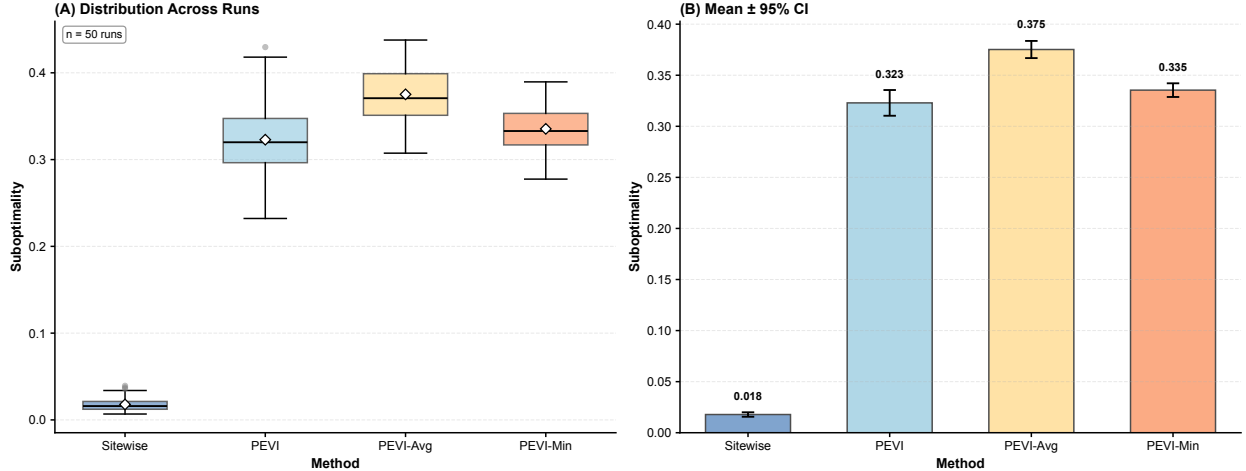


Figure 1: **Comparison of suboptimality between the proposed Sitewise algorithm and benchmark methods.** (A) Distribution of suboptimality over 50 runs. (B) Mean and 95% confidence intervals of the average suboptimality values. The Sitewise method demonstrates significantly lower suboptimality and higher stability.

specific distributional shifts, leading to a marked drop in performance in the most challenging environments. Similarly, both per-site PEVI methods exhibit high suboptimality. This observation is likely due to the limited sample size at each site, leading to high variance in local estimators. In addition, the absence of information sharing across sites appears to prevent these methods from learning a robust policy.

Furthermore, Figure 1 highlights the statistical stability of Algorithm 1. The estimator demonstrates remarkably lower variance across simulation runs compared to the benchmarks. This suggests that the proposed Algorithm 1 can balance the bias-variance trade-off effectively, providing a robust estimator even in the presence of site-specific heterogeneity.

4.2 Convergence Rate

In this subsection, we analyze the convergence behavior of Algorithm 1 and empirically validate the theoretical upper bound of suboptimality derived in Corollary 4.

To construct a challenging scenario that reflects the theoretical lower bound, we adopt the hard instance design from (Jin et al., 2021), extending it to the multi-site setting. Specifically, for each site $k \in [K]$, we consider an MDP with a finite horizon H and a small state space

$\mathcal{S} = \{s_0, s_1, s_2\}$. The action space is $\mathcal{A} = \{b_1, \dots, b_A\}$, where $|\mathcal{A}| = A \geq 3$.

The transition dynamics are defined as follows: at the fixed initial state s_0 , taking action a leads to the “good” absorbing state s_1 with probability $P(s_1 | s_0, a)$ and the “bad” absorbing state s_2 with probability $1 - P(s_1 | s_0, a)$. Specifically, at step $h = 1$, for each site $k \in [K]$, the transition probabilities are defined as follows:

$$\begin{aligned} P_1^k(s_1 | s_0, b_1) &= p_1^k, & P_1^k(s_2 | s_0, b_1) &= 1 - p_1^k, \\ P_1^k(s_1 | s_0, b_2) &= p_2^k, & P_1^k(s_2 | s_0, b_2) &= 1 - p_2^k, \\ P_1^k(s_1 | s_0, b_j) &= p_3^k, & P_1^k(s_2 | s_0, b_j) &= 1 - p_3^k, \quad \forall j \in \{3, \dots, A\}. \end{aligned}$$

The reward is deterministic and depends solely on the current state: $r(s_1) = 1$ and $r(s_2) = 0$. Once the agent enters s_1 or s_2 , it remains there with the corresponding reward for subsequent steps (absorbing states). We define the feature map $\phi(s, a)$ of dimension $d = A + 2$ as:

$$\begin{aligned} \phi(s_0, b_j) &= (\mathbf{e}_j, 0, 0)^\top \in \mathbb{R}^{A+2}, \quad \forall j \in [A], \\ \phi(s_1, a) &= (\mathbf{0}_A, 1, 0)^\top \in \mathbb{R}^{A+2}, \quad \forall a \in \mathcal{A}, \\ \phi(s_2, a) &= (\mathbf{0}_A, 0, 1)^\top \in \mathbb{R}^{A+2}, \quad \forall a \in \mathcal{A}, \end{aligned}$$

where \mathbf{e}_j denotes the j -th standard basis vector and $\mathbf{0}_A$ is the zero vector in \mathbb{R}^A .

To verify the convergence rate, we scale the difficulty of the problem instance inversely with the sample size. Let n_1^k and n_2^k denote the number of trajectories in site k where the first action corresponds to b_1 and b_2 , respectively:

$$n_j^k = \sum_{\tau=1}^{N_k} \mathbf{1} \left\{ a_1^{(k, \tau)} = b_j \right\}, \quad \text{for } j \in \{1, 2\}.$$

We set the gap parameter δ^k as:

$$\delta^k = \frac{1}{8} \sqrt{\frac{3}{2(n_1^k + n_2^k)}},$$

and define the transition parameters as:

$$p_1^k = 0.5 + \delta^k, \quad p_2^k = 0.5 - \delta^k, \quad \text{and} \quad p_3^k = \min\{p_1^k, p_2^k\}.$$

Under this construction, the robust optimal policy π^* is deterministic and selects action b_1 at the initial state s_0 (since $p_1^k > 0.5 > p_2^k$ for all sites). The robust suboptimality, as defined

in (9), can then be expressed as:

$$\begin{aligned}\text{SubOpt}(\widehat{\pi}; s_0) &= V_1^*(s_0) - V_1^{\widehat{\pi}}(s_0) \\ &= (H-1) \cdot \left[\min_{k \in [K]} p_1^k - \min_{k \in [K]} P_1^k(s_1 \mid s_0, \widehat{\pi}_1(s_0)) \right],\end{aligned}$$

where $\widehat{\pi}_1(s_0)$ denotes the action selected by the learned policy $\widehat{\pi}$ at the first step.

In our experiments, the hyperparameters for Algorithm 1 are configured as follows: the ridge regularization coefficient is set to $\lambda = 1$, the confidence level for uncertainty quantification is $\xi = 0.05$, and the scaling constant in the penalty term is $c = 5 \times 10^{-4}$. The problem instance consists of $K = 4$ sites with an action space size of $A = 7$ and a horizon length of $H = 40$. To empirically verify the theoretical convergence rate, we generate datasets across a spectrum of sample sizes, specifically varying the minimum sample size N_{\min} over the set $\{50, 100, 500, 1000, 2000, 5000, 8000\}$.

To ensure statistical reliability, we perform $R = 50$ independent trials. We report the mean suboptimality versus N_{\min} on a log-log scale, where error bars indicate the 95% confidence interval across trials. Furthermore, to quantify the scaling laws, we perform linear regression in the log-log space. The reported slopes are the fitted scaling exponents from the log-log regression, with 95% confidence intervals. Meanwhile, we demonstrate the results of Value Gap, which is defined as:

$$\text{ValGap}(s_0) = V_1^*(s_0) - \widehat{V}_1(s_0),$$

where $\widehat{V}_1(s_0)$ denotes the pessimistic value estimated by Algorithm 1 at the initial state.

Figure 2 illustrates the scaling laws of the Algorithm 1, showing that both suboptimality and the Value Gap decay monotonically with increasing minimum sample size N_{\min} . The linear trends in the log-log plots confirm a power-law relationship. Notably, the observed slope for suboptimality is approximately -0.45 , which aligns closely with the theoretical rate of $O(N_{\min}^{-1/2})$ given in Corollary 4. This close agreement supports our theoretical analysis and indicates that the derived bound captures the essential learning dynamics of our algorithm in this setting.

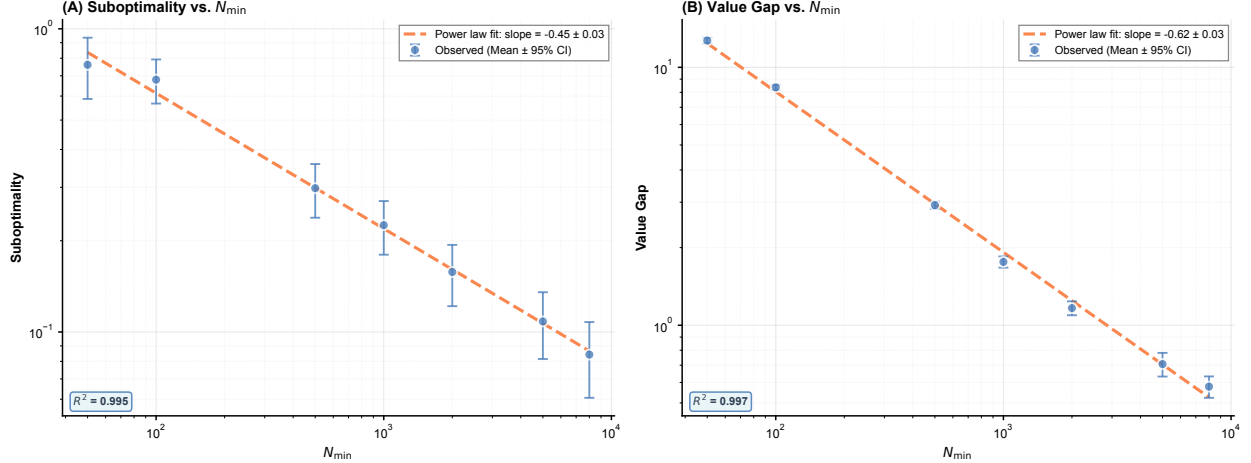


Figure 2: **Scaling relationships between minimum sample size and performance metrics.** (A) Suboptimality decreases with N_{\min} following a power law (slope = -0.45 ± 0.03 , $R^2 = 0.995$). (B) Value Gap shows similar power-law decay (slope = -0.62 ± 0.03 , $R^2 = 0.997$). Data points represent the mean \pm 95% CI across independent runs. Dashed lines show fitted power-law relationships in log-log space.

4.3 The Necessity of the Pessimism Penalty

In this section, we investigate the critical role of the pessimism penalty of Algorithm 1. We design a specific test case to compare the convergence behaviors of our algorithm with ($c > 0$) and without ($c = 0$) the penalty term.

In this experiment, we adopt a similar setup to that in Section 4.1 but construct a specific ‘‘hard’’ instance to challenge the estimator. We restrict the action space to $|\mathcal{A}| = 2$, consisting of a *safe action* and a *trap action*. The expected rewards are set to 0.70 and 0.65, respectively.

To simulate a deceptive scenario, we employ a high-variance reward distribution, which increases the likelihood that the empirical mean of the *trap* action exceeds that of the optimal (*safe*) one due to finite-sample noise. Furthermore, we enforce imbalanced data coverage, where the trap action is sampled a fixed, limited number of times (e.g., typically < 10), regardless of the dataset size.

The hyperparameters for Algorithm 1 are set as follows: the ridge regularization coefficient is set to $\lambda = 1 \times 10^{-5}$, the confidence level for uncertainty quantification is $\xi = 0.05$,

and the scaling constant in the penalty term is set to be $c \in \{0, 5 \times 10^{-4}, 1 \times 10^{-3}\}$. The problem instant consists of $K = 3$ sites with $A = 2$ actions and a horizon length of $H = 7$. In order to compare the performance of different choice of c , we generate datasets across a spectrum of sample sizes, where the minimum sample size changes over the set $\{20, 200, 2000, 20000, 200000, 2000000\}$.

We conduct $R = 50$ independent trials using different random seeds. In each trial, we compute the average suboptimality over $m = 200$ initial states selected uniformly from \mathcal{S} . Then we report the mean suboptimality versus N_{\min} on a log-log scale, with error bars indicating the 95% confidence interval across trials. Additionally, we perform linear regression in the log-log space to quantify the convergence rates associated with different values of c .

Figure 3 demonstrates the critical role of the pessimism penalty. When $c = 0$, Algorithm 1 reduces to a greedy approach and fails to converge efficiently, as evidenced by the plateau in suboptimality (slope ≈ -0.15). In contrast, with $c = 0.0005$ and $c = 0.001$, the algorithm identifies the true optimal policy efficiently, resulting in fast convergence rates. These results empirically validate the necessity of the pessimism penalty.

This observed failure of the greedy estimator ($c = 0$) stems from the imbalanced coverage of the dataset. The greedy estimator tends to overfit to finite-sample noise, specifically the few “lucky” high rewards observed from the high-variance trap action. In contrast, setting $c > 0$ activates the uncertainty quantification mechanism. The penalty term grows large for the sparsely sampled trap action, effectively counteracting the deceptively high empirical mean caused by finite-sample noise.

5 Discussion

In this paper, we focus on group-linear DRMDPs and propose an offline algorithm. Our formulation relies on the d -rectangular uncertainty set, which relaxes the original non-rectangular cross-site convex hull structure. We acknowledge that this approximation expands the feasible set for the adversary, potentially leading to conservative estimation. However, this design is necessary to circumvent the NP-hardness when optimizing over the non-rectangular structure. Future work can explore tighter approximations that better balance the trade-off between accuracy and computational tractability.

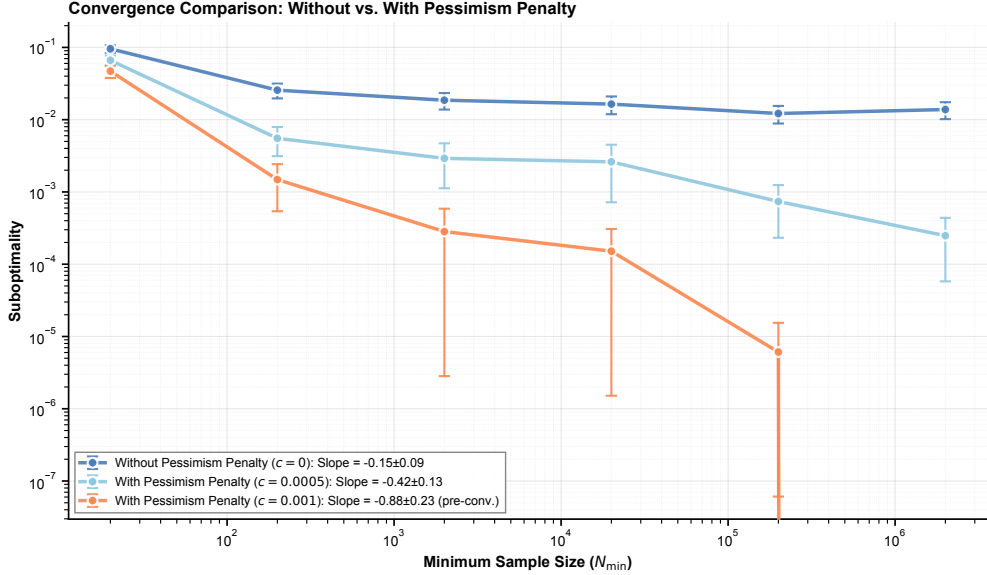


Figure 3: **Convergence comparison between estimators without and with pessimism penalty.** The estimator without penalty ($c = 0$, dark blue) fails to converge efficiently, exhibiting a plateau with a flat slope (-0.15 ± 0.09). Incorporating the pessimism penalty ($c > 0$) restores the power-law decay in suboptimality. **Note:** For the strong penalty case ($c = 0.001$, orange), the algorithm achieves exact optimal policy (zero suboptimality) at the largest sample size ($N_{\min} = 2 \times 10^6$). The reported slope (-0.88 ± 0.23) is thus calculated using the first 5 (pre-convergence) data points.

In addition, our proposed method relies on the linear structure within each site. While this formulation mainly facilitates the theoretical analysis and robust planning, it may not hold exactly in real-world applications. In practice, designing an optimal feature map is non-trivial and model misspecification can inevitably result in estimation bias. Consequently, a significant direction for future work is to incorporate representation learning to automatically learn an appropriate feature map.

Acknowledgment

The work described in this paper was partially supported by a grant from the ANR/RGC Joint Research Scheme sponsored by the Research Grants Council of the Hong Kong Special Administrative Region, China and French National Research Agency (Project No. A-

References

Blanchet, J., M. Lu, T. Zhang, and H. Zhong (2023). Double Pessimism is Provably Efficient for Distributionally Robust Offline Reinforcement Learning: Generic Algorithm and Robust Partial Coverage. In *Advances in Neural Information Processing Systems*, Volume 36, pp. 66845–66859. Curran Associates, Inc.

Goyal, V. and J. Grand-Clément (2023). Robust Markov Decision Processes: Beyond Rectangularity. *Mathematics of Operations Research* 48(1), 203–226.

Iyengar, G. N. (2005). Robust Dynamic Programming. *Mathematics of Operations Research* 30(2), 257–280.

Jin, C., Z. Yang, Z. Wang, and M. I. Jordan (2020). Provably efficient reinforcement learning with linear function approximation. In *Proceedings of Thirty Third Conference on Learning Theory*, Volume 125 of *Proceedings of Machine Learning Research*, pp. 2137–2143. PMLR.

Jin, Y., Z. Yang, and Z. Wang (2021). Is Pessimism Provably Efficient for Offline RL? In *Proceedings of the 38th International Conference on Machine Learning*, Volume 139 of *Proceedings of Machine Learning Research*, pp. 5084–5096. PMLR.

Kidambi, R., A. Rajeswaran, P. Netrapalli, and T. Joachims (2020). MOReL: Model-Based Offline Reinforcement Learning. In *Advances in Neural Information Processing Systems*, Volume 33, pp. 21810–21823. Curran Associates, Inc.

Kumar, A., A. Zhou, G. Tucker, and S. Levine (2020). Conservative Q-Learning for Offline Reinforcement Learning. In *Advances in Neural Information Processing Systems*, Volume 33, pp. 1179–1191. Curran Associates, Inc.

Levine, S., A. Kumar, G. Tucker, and J. Fu (2020). Offline Reinforcement Learning: Tutorial, Review, and Perspectives on Open Problems. arXiv preprint arXiv:2005.01643.

Li, M., D. Kuhn, and T. Sutter (2025). Towards Optimal Offline Reinforcement Learning. arXiv preprint arXiv:2503.12283.

Li, Y. (2025). Computational Hardness of Static Distributionally Robust Markov Decision Processes. arXiv preprint arXiv:2511.02224.

Liu, Z. and P. Xu (2025). Linear Mixture Distributionally Robust Markov Decision Processes. arXiv preprint arXiv:2505.18044.

Ma, X., Z. Liang, J. Blanchet, M. Liu, L. Xia, J. Zhang, Q. Zhao, and Z. Zhou (2023). Distributionally Robust Offline Reinforcement Learning with Linear Function Approximation. arXiv preprint arXiv:2209.06620.

Pricope, T.-V. (2021). Deep Reinforcement Learning in Quantitative Algorithmic Trading: A Review. arXiv preprint arXiv:2106.00123.

Sagawa, S., P. W. Koh, T. B. Hashimoto, and P. Liang (2020). Distributionally Robust Neural Networks for Group Shifts: On the Importance of Regularization for Worst-Case Generalization. arXiv preprint arXiv:1911.08731.

Uehara, M. and W. Sun (2021). Pessimistic Model-based Offline Reinforcement Learning under Partial Coverage. arXiv preprint arXiv:2107.06226.

Wang, Z., N. Si, Z. Guo, and M. Liu (2024). Inference for Stable Variable Importance across Multi-source Domains via Adversarial Learning. arXiv preprint arXiv:2409.07380.

Yu, T., G. Thomas, L. Yu, S. Ermon, J. Y. Zou, S. Levine, C. Finn, and T. Ma (2020). MOPO: Model-based Offline Policy Optimization. In *Advances in Neural Information Processing Systems*, Volume 33, pp. 14129–14142. Curran Associates, Inc.

Zhang, C., Z. Jia, G. K. Atia, S. He, and Y. Wang (2025). Pessimism Principle Can Be Effective: Towards a Framework for Zero-Shot Transfer Reinforcement Learning. arXiv preprint arXiv:2505.18447.

Zhang, X., Y. Chen, X. Zhu, and W. Sun (2022). Corruption-robust Offline Reinforcement Learning. In *Proceedings of The 25th International Conference on Artificial Intelligence and Statistics*, Volume 151 of *Proceedings of Machine Learning Research*, pp. 5757–5773. PMLR.

Zhou, D., Y. Zhang, A. Sonabend-W, Z. Wang, J. Lu, and T. Cai (2024). Federated Offline Reinforcement Learning. *Journal of the American Statistical Association* 119(548), 3152–3163.